

# A search for neutrino signal from dark matter annihilation in the center of the Milky Way with Baikal NT200

A.D. Avrorin<sup>a</sup>, A.V. Avrorin<sup>a</sup>, V.M. Aynutdinov<sup>a</sup>, R. Bannasch<sup>g</sup>, I.A. Belolaptikov<sup>b</sup>, D.Yu. Bogorodsky<sup>c</sup>, V.B. Brudanin<sup>b</sup>, N.M. Budnev<sup>c</sup>, I.A. Danilchenko<sup>a</sup>, S.V. Demidov<sup>a,\*</sup>, G.V. Domogatsky<sup>a</sup>, A.A. Doroshenko<sup>a</sup>, A.N. Dyachok<sup>c</sup>, Zh.-A.M. Dzhilkibaev<sup>a</sup>, S.V. Fialkovsky<sup>e</sup>, A.R. Gafarov<sup>c</sup>, O.N. Gaponenko<sup>a</sup>, K.V. Golubkov<sup>a</sup>, T.I. Gress<sup>c</sup>, Z. Honz<sup>b</sup>, K.G. Kebkal<sup>g</sup>, O.G. Kebkal<sup>g</sup>, K.V. Konischev<sup>b</sup>, A.V. Korobchenko<sup>c</sup>, A.P. Koshechkin<sup>a</sup>, F.K. Koshel<sup>a</sup>, A.V. Kozhin<sup>d</sup>, V.F. Kulepov<sup>e</sup>, D.A. Kuleshov<sup>a</sup>, V.I. Ljashuk<sup>a</sup>, M.B. Milenin<sup>e</sup>, R.A. Mirgazov<sup>c</sup>, E.R. Osipova<sup>d</sup>, A.I. Panfilov<sup>a</sup>, L.V. Pan'kov<sup>c</sup>, E.N. Pliskovsky<sup>b</sup>, M.I. Rozanov<sup>f</sup>, E.V. Rjabov<sup>c</sup>, B.A. Shaybonov<sup>b</sup>, A.A. Sheifler<sup>a</sup>, M.D. Shelepov<sup>a</sup>, A.V. Skurihin<sup>d</sup>, A.A. Smagina<sup>b</sup>, O.V. Suvorova<sup>a,\*</sup>, V.A. Tabolenco<sup>c</sup>, B.A. Tarashansky<sup>c</sup>, S.A. Yakovlev<sup>g</sup>, A.V. Zagorodnikov<sup>c</sup>, V.A. Zhukov<sup>a</sup>, V.L. Zurbanov<sup>c</sup>

<sup>a</sup>*Institute for Nuclear Research, 60th October Anniversary pr. 7A, Moscow 117312, Russia*

<sup>b</sup>*Joint Institute for Nuclear Research, Dubna 141980, Russia*

<sup>c</sup>*Irkutsk State University, Irkutsk 664003, Russia*

<sup>d</sup>*Skobeltsyn Institute of Nuclear Physics MSU, Moscow 119991, Russia*

<sup>e</sup>*Nizhni Novgorod State Technical University, Nizhni Novgorod 603950, Russia*

<sup>f</sup>*St. Petersburg State Marine University, St. Petersburg 190008, Russia*

<sup>g</sup>*EvoLogics GmbH, Berlin, Germany*

---

## Abstract

We reanalyze the dataset collected during the years 1998–2003 by the deep underwater neutrino telescope NT200 in the lake Baikal with the low energy threshold (10 GeV) in searches for neutrino signal from dark matter annihilations near the center of the Milky Way. Two different approaches are used in the present analysis: counting events in the cones around the direction towards the Galactic Center and the maximum likelihood method. We assume that the dark matter particles annihilate dominantly over one of the annihilation channels  $b\bar{b}$ ,  $W^+W^-$ ,  $\tau^+\tau^-$ ,  $\mu^+\mu^-$  or  $\nu\bar{\nu}$ . No significant excess of events towards the Galactic Center over expected neutrino background of atmospheric origin is found and we derive 90% CL upper limits on the annihilation cross section of dark matter.

*Keywords:*

---

## 1. Introduction

Today all cosmological and astrophysical observations are successfully explained within a paradigm of the standard cosmological model ( $\Lambda$ CDM) stating that the most of the energy density of the Universe is stored in the dark energy or cosmological constant ( $\Lambda$ , about 68%) and non-baryonic cold dark matter (CDM, about 27%). Unambiguous presence of the latter component is confirmed by measurements of galaxy rotation curves [1], weak gravitational lensing of distant objects like galaxy clusters [2], measurements of properties of cosmic microwave background [3, 4, 5], analysis of structure formation [6] and nucleosynthesis [7] (see also Ref. [8] for a review).

One of the most favorable ideas for explaining dark matter (DM) phenomena is Weakly Interacting Massive Particles or WIMPs [9]. In this scenario predicted by several classes of models of new physics [10, 11],

---

\*Corresponding authors

*Email addresses:* demidov@ms2.inr.ac.ru (S.V. Demidov), suvorova@cpc.inr.ac.ru (O.V. Suvorova)

these particles are supposed to be in thermal equilibrium in the early Universe and can annihilate into Standard Model particles. But as the Universe was expanding and cooling down, the annihilation processes ceased and number density of the dark matter particles became frozen out at some value which is determined by their annihilation cross section. Thus, at least in the WIMP scenario one can expect some signal from the dark matter annihilations towards the directions of local overpopulation of these particles. The Galactic Center (GC) of the Milky Way is one such direction.

Two types of messengers from DM annihilation signal in the Galactic Center, i.e. gamma rays and neutrinos, are expected to be detected by the telescopes. They both originate in the same energy ranges (GeV–TeV for WIMPs) in decays of particles produced in kinematically allowed dark matter annihilation channels. Several analyses of diffuse gamma-rays from the FERMI-LAT dataset (pass 7) point out on an evidence for central and spatially extended excess toward the Galactic Center (GCE). Large astrophysical uncertainties to the background of diffuse gamma-radiation in the Galaxy generate ambiguous interpretations of the GCE. Among the scenarios explaining the GCE there have been discussed possibilities of unresolved conventional astrophysical gamma-ray sources, e.g. millisecond pulsars [12] as well as different extensions of the Standard Model with dark matter particles annihilating in the MW halo [13] (for a review see e.g. Ref. [14]). The analysis performed in Ref. [13] which uses filtered emissions from individual point sources like globular clusters and millisecond pulsars detected by the FERMI-LAT, supports a DM signal from annihilations either into  $b\bar{b}$  channel with dark matter particle of the mass about 30–60 GeV or into  $\tau^+\tau^-$  channel for the masses in 5–15 GeV range. The annihilation cross section is found to be about  $10^{-26}\text{cm}^3/\text{s}$  which is close to the value predicted in the scenario of WIMPs annihilation in the early Universe. The latest analysis of the FERMI-LAT dataset (pass 8) [15] shows some tension in consistency with the dark matter interpretations of the GCE, related to the dark matter density profile and the value of local dark matter density.

The operating neutrino telescopes have not yet observed a signal from the dark matter annihilations in the GC over expected atmospheric neutrino background, see recent analyses from the ANTARES [16], IceCube [17] and Super-Kamiokande [18] collaborations. In this paper we analyze the dataset of upward going muons produced by neutrinos in the lake Baikal and measured with the NT200 telescope for a period between April of 1998 to February of 2003 in search for an excess in the directions near the GC. We focus on the dark matter particles with masses from 30 GeV to 10 TeV annihilating dominantly into one of the following benchmark annihilation channels:  $b\bar{b}$ ,  $W^+W^-$ ,  $\tau^+\tau^-$ ,  $\mu^+\mu^-$  and also flavor-symmetric neutrino channel  $\nu\bar{\nu}$ . Two independent analyses of the data are performed and consistent results are found. Finally, we obtain upper limits on the dark matter annihilation cross section for these annihilation channels. Also we discuss influence of systematic uncertainties on the obtained results.

## 2. Experiment and data sample

The NT200 is a deep underwater neutrino telescope in lake Baikal which began data taking in 1993. This detector was the first that proved the method of study of high energy muons, which come from top or bottom hemisphere across a large volume of natural water, by recording their Cherenkov radiation [19]. Lake Baikal deep water is characterized by the absorption length of  $L_{abs}(480\text{ nm}) = 20 - 24\text{ m}$ , scattering length of  $L_{sc} = 30 - 70\text{ m}$  and strongly anisotropic scattering function with the mean cosine of the scattering angle of 0.85–0.9. The Cherenkov light of relativistic particles is recorded at appropriate wavelengths by an array of optical modules (OMs) which are time-synchronized and energy-calibrated by artificial light pulses. At 1 km water depth, the muon flux from cosmic ray interactions in the upper atmosphere is about one million times higher than the flux of upward going muons initiated by neutrino interactions in the water and rock below the array. Selection of clean neutrino event sample of true upward going muons is a major challenge which requires highly efficient rejection of misreconstructed downward moving muons. The NT200 instrumentation volume encloses 100 Ktons placed in the southern basin of the lake Baikal, at the distance of 3.5 km off the shore and at the depth of 1.1 km. In Fig. 1 (on left), the visibility over declinations for the NT200 site located at  $51.83^\circ$  of Northern latitude is shown. Here we account for its dead time when the detector had to be upgraded in the winter expeditions [20]. Note, that in April 2015 there has been deployed a new larger detector [21] operating now at this place as a demonstration cluster of about 2 Mton size for a

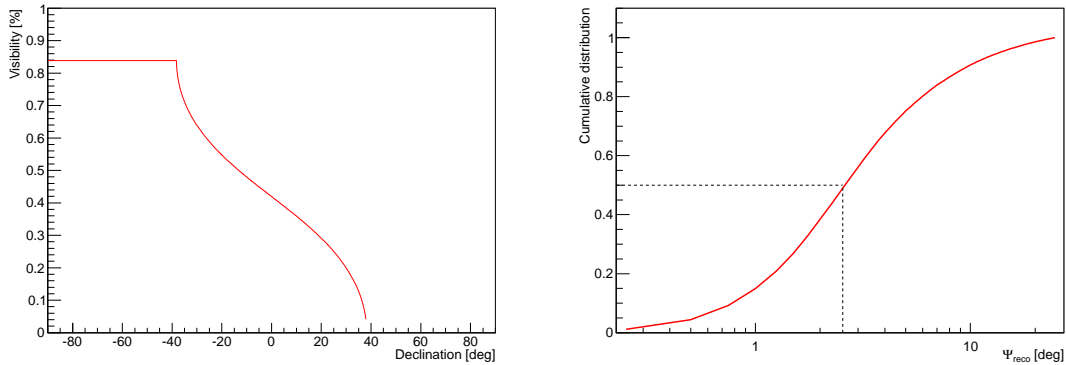


Figure 1: Left: The NT200 visibility as a function of the declination. Right: The cumulative distribution of the reconstruction angle  $\Psi_{reco}$  for the NT200 data analysis. The black-dotted line indicates the median value.

future Gigaton volume detector [22]. Sensitivity of the future experiment to the DM annihilation signal from the GC has been discussed in Ref. [23]. The NT200 configurations, functional systems, calibration methods and software for muon track reconstruction have been described elsewhere [20, 24, 25, 26, 27, 28]. The detector consists of 192 optical modules arranged pairwise on 8 strings of 68.75 m length: seven peripheral strings and a central one. The distance between the nearest strings is 21.5 m. Each OM contains hybrid photodetector QUASAR-370, a photo multiplier tube (PMT) with 37-cm diameter. To suppress background from dark noise, two PMTs of a pair are switched in coincidence within the time window of 15 ns. Present analysis is based on the data collected between April of 1998 and February of 2003, with in total 2.76 live years, and taken with the muon trigger. The trigger requires  $N_{hit} \geq n$  within 500 ns, where hit refers to a pair of fired OMs coupled in a *channel*. Typically the value of  $n$  is set to 3 or 4. We use the same dataset and Monte Carlo (MC) sample as in Ref. [29]. The detector response to the atmospheric muons and neutrinos has been obtained with MC simulations based on standard codes CORSIKA [30] and MUM [31] using the Bartol atmospheric  $\nu$  flux [32]. To distinguish upward and downward going muons on one-per-million mis-assignment level, a filter with several levels of quality cuts was developed for the atmospheric neutrino ( $\nu_{atm}$ ) analysis [33]. The atmospheric muons which have been mis-reconstructed as upward-going particles are the main source of the background in the search for neutrino induced upward-going muons. The offline filter which requires at least 6 hits on at least 3 strings ("6/3") selects about 40% of all triggered events. At this level the r.m.s. mismatch angle  $\psi_{reco}$  between the direction of incoming muon and its reconstructed value is about  $14.1^\circ$  for the  $\nu_{atm}$ -sample. To get the best possible estimator for the direction, we use multiple start guesses for the  $\chi^2$  minimization [28]. For the final choice of the local minimum of  $\chi^2$ , we use quality parameters which are not related to the time information. The quality cuts are applied to variables like the number of hit channels,  $\chi^2/d.o.f.$ , the probability of fired channels to have been hit or not and the actual position of the track with respect to the detector center. To improve the signal-to-background ratio we use only events with the reconstructed zenith angle  $\Theta > 100^\circ$ . All the cuts provide rejection factor for the atmospheric muons of about  $10^{-7}$ , resulting in the neutrino energy threshold of about 10 GeV, dispersion of  $4.5^\circ$  for the distribution of mismatch angles and the median value  $2.5^\circ$  as it is seen in Fig. 1 (right) (for more details see Ref. [28, 33]). In Fig. 2 we show the arrival directions of reconstructed muons in galactic coordinates and cones around the GC with opening angles  $20^\circ$ ,  $5^\circ$  and  $2.5^\circ$  containing 31, 2 and 2 observed events, respectively. In the next Section, we discuss expected signal from the dark matter annihilations in our Galaxy and background from the atmospheric neutrinos.

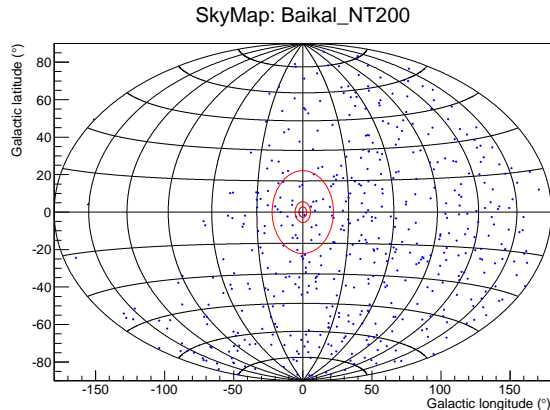


Figure 2: The NT200 sample of neutrino events in galactic coordinates

### 3. Signal and background

Neutrino flux at the Earth from the dark matter annihilations in the Galactic Center from a particular direction has the following form

$$\frac{d\phi_\nu}{dE_\nu d\Omega} = \frac{\langle\sigma_a v\rangle}{2} J_a(\psi) \frac{R_0 \rho_0^2}{4\pi m_{DM}^2} \frac{dN_\nu}{dE_\nu}, \quad (1)$$

where  $\langle\sigma_a v\rangle$  is the annihilation cross section averaged over velocity distribution of the dark matter particles at present epoch and  $dN_\nu/dE_\nu$  is the (anti)neutrino energy spectrum. The astrophysical factor  $J_a(\psi)$  can be parametrized as a function of angular distance  $\psi$  from the GC to the chosen direction and has the form

$$J_a(\psi) = \int_0^{l_{max}} \frac{dl}{R_0} \frac{\rho^2 \left( \sqrt{R_0^2 - 2rR_0 \cos \psi + r^2} \right)}{\rho_0^2}. \quad (2)$$

Here  $R_0$  is the distance from the GC to the Solar System,  $\rho_0$  is the local dark matter density and integration goes along line-of-sight till  $l_{max}$  which is much larger than the size of the Milky Way. Several different models are used to describe the dark matter density distribution of our Galaxy, see e.g. Refs. [34, 35, 36, 37, 38]. Numerical N-body simulations [39] show that dark matter form an almost spherical halo. Simulations without baryons predict cuspy profiles. However, inclusion of the baryons can change these conclusions and N-body simulations being limited in number of particles can not resolve small area around the center of galaxy, so the main uncertainty in the profile comes from this region. At the same time the signal from annihilations is proportional to the square of the dark matter density, see Eq. (1). So, this part of astrophysical input is the main theoretical uncertainty for the signal from DM annihilations in the Galaxy. Direct observational data of the Milky Way can not resolve this uncertainty, because the part of our Galaxy within the Solar System circle is dominated by baryons, so the influence of the dark matter within this circle on motion of astrophysical objects is small. Even the local dark matter density is known with a large uncertainty  $0.2\text{--}0.6 \text{ GeV}\cdot\text{cm}^{-3}$ . Moreover, one can not exclude a possibility that dark matter can form clumps in our Galaxy and that the signal from a particular directions can be increased by the presence of a clump along line-of-sight [40]. We will present the final results for Navarro-Frenk-White (NFW) [34, 35] model of the DM density profile and compare them with more cuspy profile in the Moore [37] model and cored profile of the Burkert [38] model. The latter one is a currently favored by the observational data [41]. All these profiles can be described as follows

$$\rho(r) = \frac{\rho_*}{\left(\delta + \frac{r}{r_*}\right)^\gamma \left[1 + \left(\frac{r}{r_*}\right)^\alpha\right]^{(\beta-\gamma)/\alpha}} \quad (3)$$

Model	$\alpha$	$\beta$	$\gamma$	$\delta$	$r_*$ , kpc	$\rho_*$ , GeV/cm <sup>3</sup>
NFW	1	3	1	0	20	0.3
Burkert	2	3	1	1	9.26	1.88
Moore	1.5	3	1.5	0	28	0.27

Table 1: Parameters of DM density profiles.

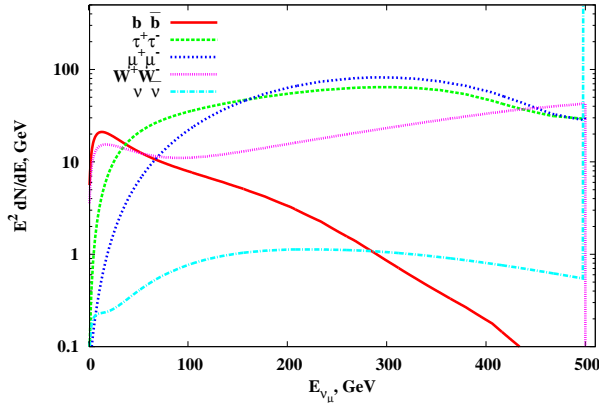


Figure 3: Neutrino  $\nu_\mu$  energy spectra at the Earth for  $m_{DM} = 500$  GeV.

with parameters presented in Table 1. The neutrino energy spectra entering Eq. (1) are determined by a particular theoretical model. In a model independent approach followed in the present study, it is assumed that the dark matter particles annihilate over particular annihilation channel with 100% branching ratio. We use  $b\bar{b}$ ,  $\tau^+\tau^-$ ,  $\mu^+\mu^-$ ,  $W^+W^-$  channels as well as  $\nu\bar{\nu} \equiv \frac{1}{3}(\nu_e\bar{\nu}_e + \nu_\mu\bar{\nu}_\mu + \nu_\tau\bar{\nu}_\tau)$  which is flavor symmetric combination of (almost) monochromatic neutrino. We consider the masses of the dark matter particles from 30 GeV to 10 TeV. For the energy spectra of these annihilation channels we use the results of Ref. [42] which include electroweak corrections important for large masses of the particles. After propagation over astrophysically large distances, neutrinos from the GC arrive at the Earth as mass states and we use the following set [43] of the oscillation parameters:  $\Delta m_{21}^2 = 7.6 \cdot 10^{-5}$  eV<sup>2</sup>,  $\Delta m_{31}^2 = 2.48 \cdot 10^{-3}$  eV<sup>2</sup>,  $\delta_{CP} = 0$ ,  $\sin^2 \theta_{12} = 0.323$ ,  $\sin^2 \theta_{23} = 0.567$ ,  $\sin^2 \theta_{13} = 0.0234$  to calculate the muon (anti)neutrino energy spectrum. We simulate neutrino propagation through the Earth to the detector level as described in [44]. Final neutrino energy spectra are presented in Fig. 3 as an example for  $m_{DM} = 500$  GeV<sup>1</sup>.

Expected angular distributions of reconstructed signal events (muons), was obtained by MC simulations. The angular spread of the signal is determined by the behaviour of the astrophysical factor  $J_a(\psi)$  for a DM density profile, angular distribution of muons from CC interactions of neutrinos for a particular annihilation channel as well as angular resolution of the telescope. The latter has been taken into account by additionally smearing the signal according to the distribution of mismatch angles obtained with MC and whose cumulative distribution is shown in Fig. 1 (on right) (instead of Gaussian distribution with dispersion equal to the angular resolution). Expected reconstructed angular distributions of the signal are presented in Fig. 4 for two opposite cases, the softest ( $b\bar{b}$ ,  $m_{DM} = 30$  GeV) and the hardest ( $\nu\bar{\nu}$ ,  $m_{DM} = 10$  TeV) neutrino energy spectra for NFW density profile.

The background for the process in question is dominated by upgoing atmospheric neutrinos. To avoid large systematic errors, typically resulting from MC simulations, in the following analysis we use the expected

<sup>1</sup> For the case of  $\nu\bar{\nu}$  channel, an unphysical width was introduced in Ref. [42]. We changed these spectra back to their physical width conserving their normalization.

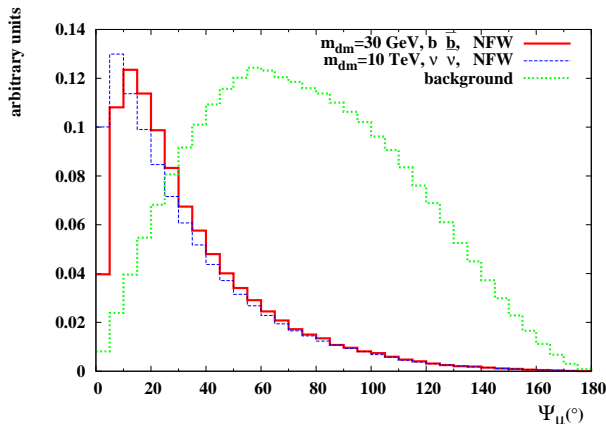


Figure 4: Expected reconstructed signal and background angular distributions.

background which is estimated from the data using their scrambling by randomization of right ascension of the events. For scrambling, we use the same full data sample of reconstructed neutrino events which has been selected with the cuts discussed in Sec.2. The form of the background obtained in this way is shown in Fig. 5 by blue histogram. In addition to the scrambling, we introduce a correction to overall normalization of this

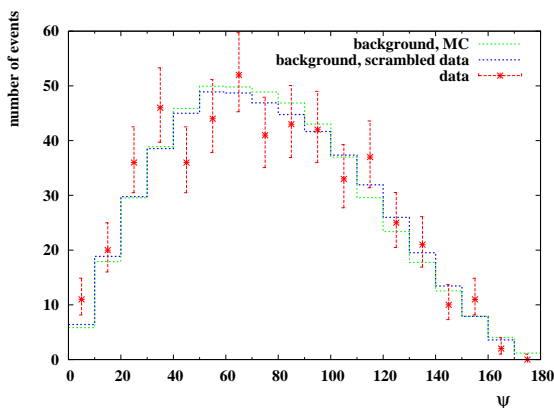


Figure 5: The data with statistical errors (red) in comparison with the background obtained using scrambling of the data (blue) and from Monte-Carlo (green).

background distribution by fitting it with the real data outside the region of expected signal contamination: we do it for  $\psi > 60^\circ$ . It is clear that using the full set of the data in this procedure we can not exclude a possible small signal contamination in our determination of the background. For cross checking, we use another procedure to obtain the shape of the background angular distribution. Namely, we simulate the reconstructed atmospheric neutrino angular distribution taking into account the visibility which is the part of observation time of a point on the sky depending on its declination. By using the visibility we simulate angular distribution of the background and impose the same cut on zenith angle to be less than 100 degrees as for real data. Again, we fit obtained shape with the data in the region  $\psi > 60^\circ$ . The comparison between two different background models is presented in Fig. 5 along with the data angular distribution.

By comparison of obtained angular distributions of signal and background with the data presented in Figs. 5 and 4, we see that there is a small excess in number of observed events toward the GC. Below we estimate statistical significance of the excess and obtain upper limits on number of signal events for each

particular DM mass and annihilation channel. Concerning the cones shown in Fig. 2, the numbers of the expected background events (observed events) inside them are 25.1 (31), 1.63 (2) and 0.42 (2).

#### 4. Data analyses

In this section we describe two different methods to analyze the data and to look for neutrino signal from the dark matter annihilations in the GC. Expected signal and background have different energy and angular distribution. Here we can use only angular information of the reconstructed events.

##### 4.1. Method A: Optimization of the cone size

For analysis *A*, we choose a cone around the direction towards the GC with half-open angle  $\Psi$  and thus obtain a counting experiment with expected number of signal  $N_S(\Psi)$  and background  $N_B(\Psi)$  as well as observed  $N_{obs}(\Psi)$  number of events. The size of the cone is optimized by choosing maximal value for signal-to-noise ratio. For blindness of the analysis we do it without use of the data in the search region. Namely, following the MRF approach [45] we construct the quantity

$$\frac{S}{N} \equiv \frac{\bar{N}_S^{90}(\Psi)}{\sqrt{N_B(\Psi)}}, \quad (4)$$

where  $\bar{N}_S^{90}(\Psi)$  is 90% CL upper limit on the number of signal neutrino events inside given cone of the size  $\Psi$  averaged over number of observed events with Poisson distribution under background only hypothesis. The optimal values of  $\Psi$  for different dark matter masses and annihilation channels are presented in Fig. 6. They

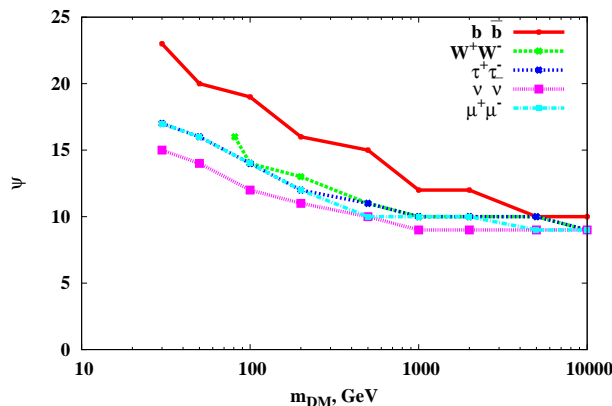


Figure 6: The optimal values of cone half-angles for different dark matter masses and annihilation channels.

vary from  $9^\circ$  for channels with hard  $\nu$  spectra to about  $23^\circ$  for annihilations with soft neutrinos. Obtained large values are due to the considerable angular spread of neutrino signal (for the NFW profile) as well due to the broad distribution of the reconstructed mismatch angles.

Inside the cones of optimal size, we set upper limits on the number of signal events  $N_S^{90}$  for a given DM mass and annihilation channel by using expected background distribution toward the GC. We apply TRolke class [46] in ROOT [47] to get the numbers taking into account systematic uncertainties to be discussed in the next Section. These upper limits are transformed into the upper limits on the dark matter annihilation cross section by using the expression for expected number of signal events from the GC direction for a live time  $T$  of observation inside a given cone

$$N(\Psi) = T \frac{\langle \sigma_a v \rangle R_0 \rho_0^2}{8\pi m_{DM}^2} J_{a,\Delta\Omega} S^{eff} \int_{E_{th}}^{m_{DM}} dE \frac{dN_\nu}{dE_\nu}. \quad (5)$$

Here  $S^{eff}$  is the effective area of the telescope averaged over neutrino energy spectrum for a particular annihilation channel

$$S^{eff} = \frac{\int dE S(E) \frac{dN_\nu}{dE_\nu}}{\int dE \frac{dN_\nu}{dE_\nu}} \quad (6)$$

within energy range from the neutrino energy threshold  $E_{th}$  to the DM mass  $m_{DM}$  and with implied sum over neutrino and antineutrino contributions. The neutrino effective area  $S^i(E_{th}, E_\nu)$  of the NT200 for a given configuration is a product of the efficiency  $\epsilon_\nu^i$  of muon reconstruction i.e. the ratio of two-dimensional angular-energy distributions of reconstructed events to simulated neutrinos, and neutrino impact area defined by MC generated volumes  $V_{MC}^i$  and the length of charged current (CC) neutrino interactions in water depending on neutrino energy  $E_\nu$ :

$$S^i(E_{th}, E_\nu, d\Omega) = V_{MC}^i \times N_A \times \rho \times \sigma^{CC}(E_\nu) \times \epsilon_\nu^i(E_{th}, E_\nu, d\Omega), \quad (7)$$

where  $i = 1, \dots, 12$  refers to twelve configurations of the NT200. During the livetime (between April of 1998 and February of 2003), the NT200 took data in various configurations, which had been changed due to failure of some groups of OMs [48]. Neglecting few-OM differences, the data can be grouped according to twelve configurations of the telescope. The values of corresponding effective areas  $S^i(E_{th}, E_\nu)$  are varied within 25% about the total effective area derived by averaging of  $S^i(E_{th}, E_\nu)$  with the fractions of data taken period in particular  $i$ -th configuration of the telescope. The weighted average value of the effective area is used in further analysis. The efficiency  $\epsilon_\nu^i(E_{th}, E_\nu, d\Omega)$  is convoluted with the visible zenith track of the GC and thus  $S(E_{th}, E_\nu)$  is entering into Eq.(7). The mean value of the generated volumes is  $V_{MC} = 4.406 \times 10^{14} \text{cm}^3$ . The value  $N_A$  is the Avogadro number,  $\rho$  is the medium density (rock or water),  $\sigma^{CC}$  is the neutrino-nucleon cross section in the CC interactions. We omit the exponential attenuation of the neutrino flux in the Earth in Eq.(7) since the shadowing effect is very weak for energies less than 10 TeV. The NT200 effective areas

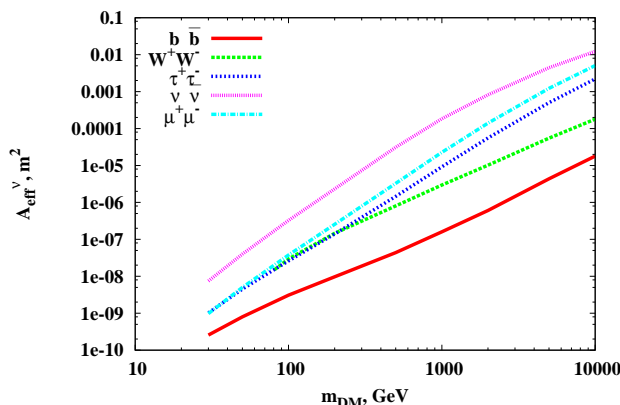


Figure 7: The effective area as a function of the mass  $m_{DM}$  of DM particle for different annihilation channels.

versus masses of dark matter particle for particular annihilation channels are shown in Fig. 7. The softest neutrino spectrum in  $b\bar{b}$  channel has the lowest effective area, while the largest area is for hard pure neutrino channel. The quantity  $J_{a,\Delta\Omega}$  in Eq. (7) is obtained by integrating the astrophysical factor  $J_a(\psi)$  over the search region with visibility  $\epsilon(\psi, \phi)$  as follows

$$J_{a,\Delta\Omega} = \int d(\cos\psi) d\phi J_a(\psi) \epsilon(\psi, \phi). \quad (8)$$

The upper limits for the dark matter annihilation cross section are set by inverting the formula (5) with respect to  $\langle\sigma_{av}\rangle$  for a given annihilation channel. Obtained results with included systematic uncertainties are shown in Fig. 8 by dashed lines in comparison with those obtained with method  $B$  (see next subsection).

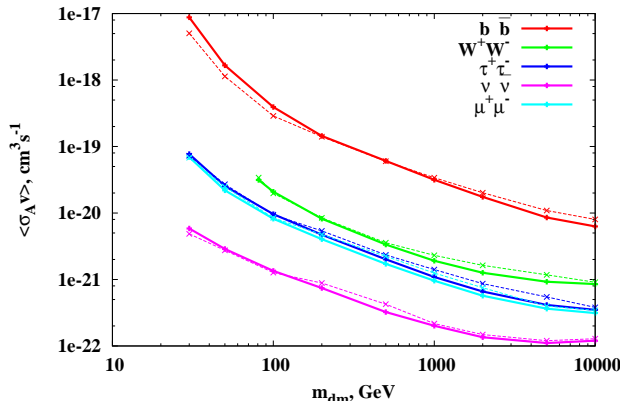


Figure 8: 90% CL upper limits on the annihilation cross section for methods *A* (dashed) and *B* (solid) assuming NFW density profile.

#### 4.2. Method B: Maximum likelihood ratio

In the analysis *B*, we construct likelihood function and use more detailed information about angular distributions of signal and background. In this case, we choose sufficiently large signal region  $\psi < 40^\circ$  for counting of the events and disregard remaining part as it is expected to be dominated by the background. Let  $f_S(\psi)$  and  $f_B(\psi)$  be expected signal and background angular distribution functions normalized in the search region. In the case of nonzero number of signal events, one expects the data will be distributed according to

$$f(\psi, N_S, N_B) = \frac{1}{N_S + N_B} (N_S f_S(\psi) + N_B f_B(\psi)). \quad (9)$$

The likelihood function is then constructed as a product of probability distributions for obtained events

$$\mathcal{L}(N_S) = \frac{(N_B + N_S)^n}{n!} e^{-(N_B + N_S)} \prod_{i=1}^n f(\psi_i, N_B, N_S) \quad (10)$$

with a multiplier with the form of the Poisson distribution accounting for fluctuations in the total number of events. Here  $n$  is the number of observed events in the search region. Systematic uncertainties for both signal and background are incorporated in the likelihood function as the nuisance parameters  $\theta \equiv \{\epsilon_S, \epsilon_B\}$  which are modeled by the Gaussian distributions. They modify the probability likelihood function as follows

$$\mathcal{L}(N_S, \epsilon_S, \epsilon_B) = \mathcal{N} \frac{(\epsilon_B N_B + \epsilon_S N_S)^n}{n!} e^{-(\epsilon_B N_B + \epsilon_S N_S) - \frac{(\epsilon_S - 1)^2}{2\sigma_S^2} - \frac{(\epsilon_B - 1)^2}{2\sigma_B^2}} \prod_{i=1}^n f(\psi_i, \epsilon_B N_B, \epsilon_S N_S), \quad (11)$$

where  $\sigma_S, \sigma_B$  are the systematic uncertainties which will be discussed in the next Section and  $\mathcal{N}$  is a normalization factor. Then, the following profile likelihood

$$\lambda(N_S) = -2 \ln \frac{\mathcal{L}(N_S, \hat{\theta}(N_S))}{\mathcal{L}(\hat{N}_S, \hat{\theta})} \quad (12)$$

is used to obtain upper limits on number of signal events. Here  $\hat{N}_S$  and  $\hat{\theta}$  are the values which give absolute maximum to the likelihood probability function, while  $\hat{\theta}(N_S)$  denotes the value of  $\theta$  in the maximum of the likelihood at fixed value of  $N_S$ . The number of observed events inside the search region  $\psi < 40$  equals 113, that is sufficiently large for the quantity  $\lambda(N_S)$  to be distributed according to the  $\chi^2$  distribution with one degree of freedom according to Wilks theorem [49, 50]. We have checked this numerically by running 10000

pseudo-experiments. Then we obtain the upper limits on the number of signal events in the search region at 90% CL by solving the equation  $\lambda(N_S^{90}) = 2.71$  [50].

To set the upper limits on the dark matter annihilation cross section for a particular channel and DM mass, we use the same inversion of the formula (5) as in the description of the analysis *A*. Numerical values of the upper limits on the annihilation cross section obtained at 90% CL with the method *B* are presented in Table 2 and in Fig. 8 (solid lines).

$m_{DM}, \text{ GeV}$	$\langle\sigma_{Av}\rangle, 10^{-21}\text{ cm}^3/\text{s}, \text{ NFW, method } B$				
	$bb$	$W^+W^-$	$\tau^+\tau^-$	$\mu^+\mu^-$	$\nu\bar{\nu}$
30	8770	–	76.9	69.3	5.86
50	1660	–	25.4	21.9	2.88
100	392	20.9	9.61	8.21	1.35
200	144	8.19	4.71	4.04	0.742
500	60.9	3.35	2.01	1.72	0.324
1000	31.6	1.91	1.09	0.957	0.201
2000	17.5	1.26	0.659	0.57	0.135
5000	8.55	0.926	0.414	0.364	0.111
10000	6.28	0.852	0.349	0.313	0.120

Table 2: 90% CL upper limits on annihilation cross section for the NFW dark matter density profiles; analyses *B*

## 5. Results and discussion

We summarize our results for annihilation cross section for different channels in plots shown in Figs. 8–11 comparing limits, obtained using methods *A* and *B*, with other experiments. Firstly, we have obtained the consistent results of both analyses. In Fig. 8 the upper limits at 90% CL on the annihilation cross sections of a DM particle for five particular channels obtained with the cone half-angle analysis (dashed lines) and with the method of maximum likelihood ratio (solid lines) are shown. Somewhat stronger upper limits are obtained with the likelihood analysis for most of the chosen dark matter masses and annihilation channels.

We run pseudo-experiments with expected background only distribution to estimate the NT200 sensitivity to the DM signal in the GC direction for the opposite cases of soft  $b\bar{b}$  and hard  $\nu\bar{\nu}$  neutrino spectra. The expected sensitivities at 90% CL are presented in Fig. 9 together with the upper limits obtained by method *B*. Colored bands in these Figures represent 68% (red) and 95% (blue) quantiles. The observed upper limits are weaker as compared to the mean values of the sensitivity, because of a small excess of events in the direction towards the GC which will be discussed later in the Section.

Neutrino telescopes are most sensitive to the pure neutrino annihilation channels. In Fig. 10 we show the NT200 results (red line) for  $\nu\bar{\nu}$  channel along with the limits on the dark matter annihilations in the GC from other neutrino experiments, the ANTARES [16], IceCube[17], Super-Kamiokande [18]. We see that in accordance with the reconstruction efficiency for sub-TeV neutrinos the NT200 upper limits obtained for  $\nu\bar{\nu}$  channel are weaker for smaller masses of the dark matter particles than those in the range of masses above TeV scale. In the latter case, they are comparable with the limits from the IceCube (analysis based on the contained events) and the Super-Kamiokande. Obviously, the low energy part of neutrino events, which are upgoing through the NT200, is difficult to distinguish from the background of atmospheric muons and it is strongly rejected by the quality cuts.

Other annihilation channels can be probed also by gamma-telescopes<sup>2</sup>. In Fig. 11 we compare upper limits at 90% CL on the  $\tau^+\tau^-$  annihilation cross section obtained with the NT200 dataset and other experiments including results by the FERMI [54] (dwarf galaxies, DES), VERITAS [55] (four dwarf galaxies), MAGIC [56]

<sup>2</sup>Here we note, that dark matter annihilations into monochromatic neutrinos are always produced with some amount of photons generated by electroweak bremsstrahlung. Thus,  $\nu\bar{\nu}$  channel can be indirectly probed with gamma-ray telescopes, see recent discussion in [53].

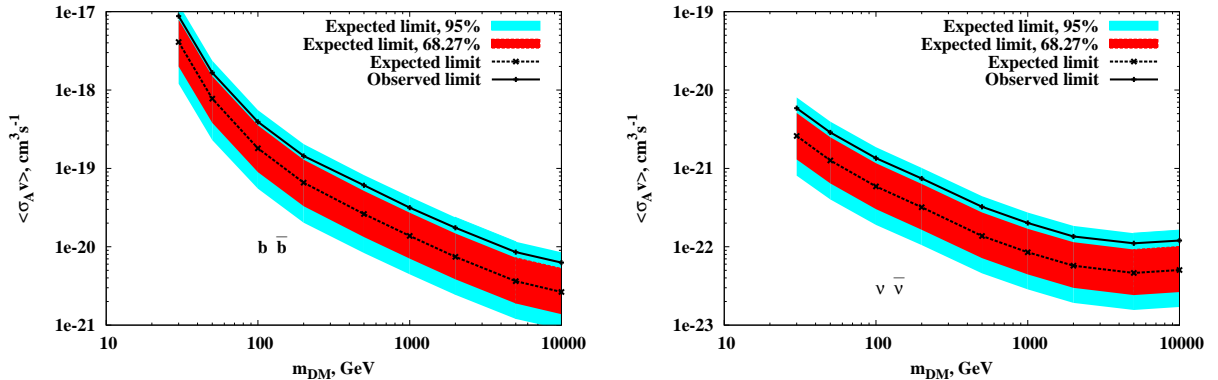


Figure 9: The upper limits on the annihilation cross section versus DM mass for channels  $b\bar{b}$  (left) and  $\nu\bar{\nu}$  (right) at 90% CL (black, solid) and the expected sensitivities (black, dashed) within its  $1\sigma$  (red band) and  $2\sigma$  (blue band) levels of statistical uncertainty.

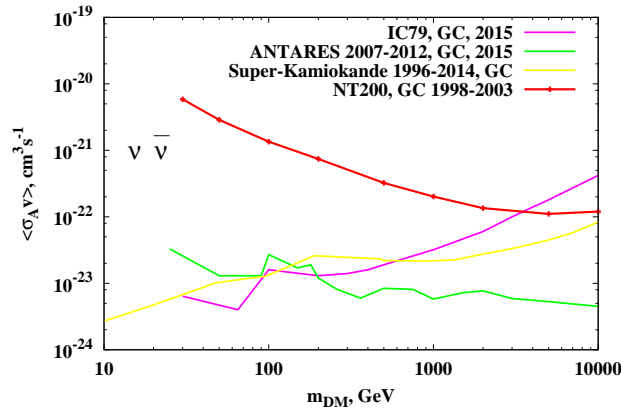


Figure 10: 90% CL upper limits on the dark matter annihilation cross section for  $\nu\bar{\nu}$  channel obtained with the NT200 dataset (red line) in this study in comparison with results from ANTARES [16], IceCube [17] and Super-Kamiokande [18].

(Segue 1), HESS [57] (dwarf galaxies), IceCube [17, 58] (GC and preliminary results for dwarf galaxies), ANTARES [16] (GC). Colorful regions show the results of DM interpretation [59] of positron excess observed by PAMELA [60] combined with the FERMI [61] and HESS [62] data. Light brown line shows the thermal relic annihilation cross section from Ref. [63].

Let us further discuss the systematic uncertainties. They include both experimental and theoretical parts. The uncertainties in the optical properties of water and in the sensitivity of the optical modules result in 30% experimental uncertainty [25, 28]. The variations of the effective area related to various telescope configurations is estimated to contribute the systematic error less than 1%. Theoretical uncertainties include present errors in the oscillation parameters and uncertainty in the neutrino-nucleon cross sections. They have been estimated using the procedure described in [29] and reach 10-12% depending on annihilation channel. We include the above uncertainties when presenting the upper limits. However, the main uncertainty comes from astrophysics. To illustrate the influence of the astrophysical uncertainty on the upper limits on the dark matter annihilation cross section, we carry out new analysis using the method *A* with the Burkert and Moore dark matter density profiles for the monochromatic neutrino annihilation channel: we make a

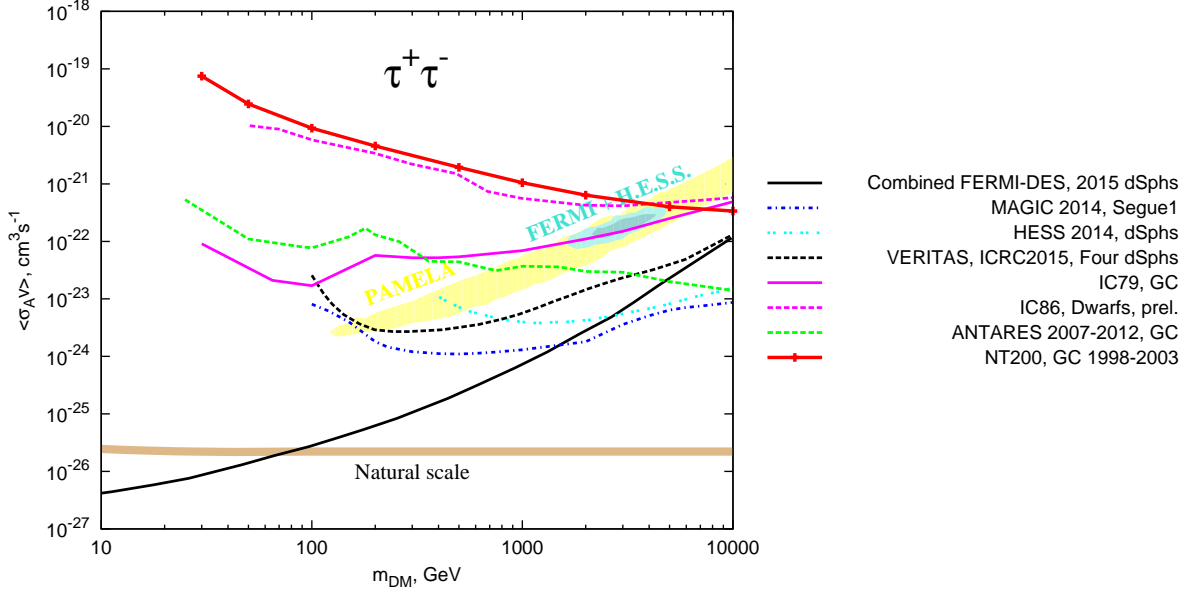


Figure 11: 90% CL upper limits on the dark matter annihilation cross section for  $\tau^+\tau^-$  channels obtained from the NT200 data in this study in comparison with results.

new MC simulation of the signal events and obtain new values of optimized cones. In Fig. 12 we show for

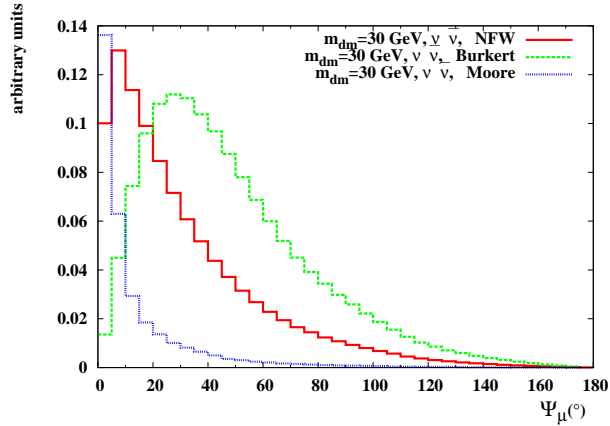


Figure 12: Reconstructed muon angular distribution from the dark matter annihilations over  $\nu\bar{\nu}$  channels for different dark matter density profiles. Relative normalizations are scaled for convenience of presentation.

illustration expected reconstructed muon angular distribution from this signal for  $\nu\bar{\nu}$  annihilation channels for different dark matter density profiles. Using optimization procedure, we found that for the Burkert profile the cone half-angle should be about  $56 - 57^\circ$  while for the Moore profile we obtain values in the range  $3 - 11^\circ$  depending on the mass of the dark matter particle and annihilation channel. Corresponding integrated  $J_a$ -factors as functions of cone size are shown in Fig. 13 for chosen dark matter density profiles. The results for upper limits on the annihilation cross section are presented in Fig. 14. We see that for very cuspy Moore profile the bounds on the annihilation cross section are improved by an order of magnitude. This is related to considerably larger values of  $J_a$ -factors even for very small opening angles as compared

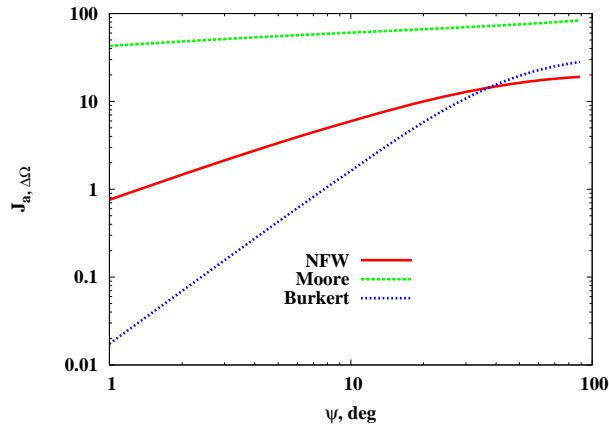


Figure 13:  $J_{a, \Delta\Omega}$  as functions of the cone half-angle  $\psi$  for different matter density profiles of the Milky Way.

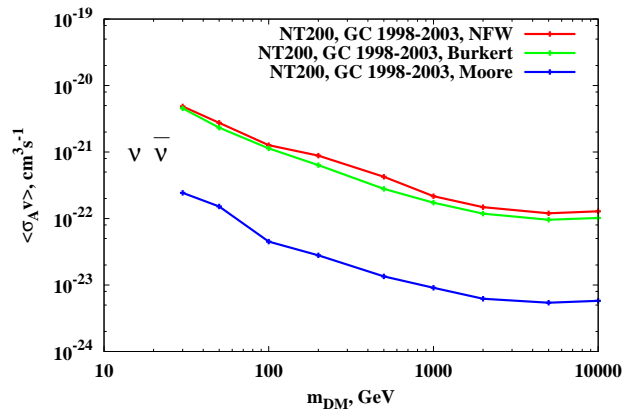


Figure 14: 90% CL upper limits on the dark matter annihilation cross section for  $\nu\bar{\nu}$  channel obtained from the NT200 data in this study for different profiles of dark matter density in the Milky Way.

to the NFW profile. At the same time the cored Burkert profile results in almost the same upper limits. In this case, the large background from new opening angle is compensated by larger astrophysical factor. We see that  $J_a$  for the case of the Burkert profile is larger than for the NFW case at  $\psi \gtrsim 37^\circ$ .

Obviously, due to observed small excess of events towards the GC we obtain a weakening of the upper limits on the dark matter annihilation cross section as compared to sensitivity. Calculating the test statistics (TS) of this excess without any systematic errors under background only hypothesis we find values 5.8 – 6.6 depending on annihilation channels. We perform a study of the influence of different systematic errors on the statistical significance of this excess. To consider astrophysical systematic uncertainty we use the NFW profile but allow corresponding parameters  $r_*$  and  $\rho_*$  vary within the following  $2\sigma$  bands

$$r_* = 16.1_{-7.8}^{+17.0} \text{ kpc}, \quad \rho_* = 0.533_{-0.354}^{+1.104} \text{ GeV/cm}^3 \quad (13)$$

taken from Ref. [41]. Their variations change the corresponding  $J_a$ -factor and thereby modify the signal both in the expected angular distribution and total flux. We include  $r_*$  and  $\rho_*$  as additional nuisance parameters in the probability likelihood function similarly to  $\epsilon_S$  in eq.(11) except that we use not Gaussian but log-normal distribution to model this uncertainty. We have found no considerable influence of the systematic uncertainty in signal (both from astrophysics and particle physics sides) on the statistical significance of

the excess. However, inclusion of systematic uncertainty in the background determination considerably brings down the values of TS to 1.4 – 1.6. Thus, we attribute this excess to a statistical fluctuation of the background only expectation within less than  $2\sigma$  level.

Finally, let us mention the uncertainty in  $J_a$ -factor related to a possible asphericity of dark matter halo [64] which can reach values up to 10%. We conservatively did not take this part of astrophysical uncertainty into account in our analysis.

## 6. Conclusions

To summarize, we studied the NT200 response to neutrinos from dark matter annihilations in the Galactic Center. We performed two independent analyses looking for an excess of neutrino events towards the GC. Both analyses show similar results. The upper limits on the dark matter annihilation cross section for 2.76 live years of observation reach values of about  $10^{-22} \text{ cm}^3\text{s}^{-1}$  at 90% CL in channel of  $\nu\bar{\nu}$  pairs when mass of the dark matter particles is heavier than 5 TeV. We studied influence of the uncertainties related to the dark matter density profile on the upper limits and found that they can result in a change of order of magnitude.

Finally, we remark that this study of neutrino signal from the GC was performed for the first time by the Baikal collaboration and we consider it as an important step towards the future analysis of the data of the ongoing GVD-project [21].

## Acknowledgments

The work of S.V. Demidov and O.V. Suvorova was supported by the RSCF grant 14-12-01430.

## References

- [1] M. Persic, P. Salucci and F. Stel, “The Universal rotation curve of spiral galaxies: 1. The Dark matter connection,” *Mon. Not. Roy. Astron. Soc.* **281** (1996) 27.
- [2] D. Clowe *et al.*, “On dark peaks and missing mass: a weak-lensing mass reconstruction of the merging cluster system A520,” *ApJ* **758**, p128, 2012.
- [3] Spergel, D. N., Verde, L., Peiris, H. V. *et al.*, “First Year Wilkinson Microwave Anisotropy Probe (WMAP) Observations: Determination of Cosmological Parameters,” *ApJS*, **148**, 175, 2003, arXiv:astro-ph/0302209.
- [4] Hinshaw, G., Larson, D., Komatsu, E., *et al.*, “Nine-Year Wilkinson Microwave Anisotropy Probe (WMAP) Observations: Cosmological Parameter Results,” 2012, arXiv:1212.5226.
- [5] Planck collaboration, P. A. R. Ade *et al.*, “Planck 2013 results. XV. CMB power spectra and likelihood,” 2013, arXiv:1303.5075.
- [6] J. R. Primack, “Dark matter and structure formation.”
- [7] K. Jedamzik and M. Pospelov, “Big Bang Nucleosynthesis and Particle Dark Matter,” *New J. Phys.* **11** (2009) 105028, [arXiv:0906.2087 [hep-ph]].
- [8] G. Bertone, D. Hooper and J. Silk, “Particle dark matter: Evidence, candidates and constraints,” *Phys. Rept.* **405** (2005) 279.
- [9] G. Steigman and M. S. Turner, “Cosmological Constraints on the Properties of Weakly Interacting Massive Particles,” *Nucl. Phys. B* **253** (1985) 375.
- [10] G. Jungman, M. Kamionkowski and K. Griest, “Supersymmetric dark matter,” *Phys. Rept.* **267** (1996) 195.
- [11] D. Hooper and S. Profumo, “Dark matter and collider phenomenology of universal extra dimensions,” *Phys. Rept.* **453** (2007) 29.
- [12] K. N. Abazajian, N. Canac, S. Horiuchi and M. Kaplinghat, “Astrophysical and Dark Matter Interpretations of Extended Gamma-Ray Emission from the Galactic Center,” *Phys. Rev. D* **90** (2014) no.2, 023526, [arXiv:1402.4090 [astro-ph.HE]].
- [13] Daylan T., Finkbeiner D.P., Hooper D., Linden T., Portillo S.K.N., Rodd N.L., Slatyer T.R., “The Characterization of the Gamma-Ray Signal from the Central Milky Way: A Compelling Case for Annihilating Dark Matter,” *FERMILAB-PUB-14-032-A*. (2014), arXiv:1402.6703.
- [14] J. Conrad, J. Cohen-Tanugi and L. E. Strigari, “WIMP searches with gamma rays in the Fermi era: challenges, methods and results,” *J. Exp. Theor. Phys.* **121** (2015) no.6, 1104, [*Zh. Eksp. Teor. Fiz.* **148** (2015) no.6, 1257], [arXiv:1503.06348 [astro-ph.CO]].
- [15] Ackerman M. *et al.* [FERMI-LAT Collab.] “Limits on Dark Matter Annihilation Signals from the Fermi LAT 4-year Measurement of the Isotropic Gamma-Ray Background”, (2015), arXiv:1501.05464.
- [16] S. Adrian-Martinez *et al.* [ANTARES Collaboration], “Search of Dark Matter Annihilation in the Galactic Centre using the ANTARES Neutrino Telescope,” *JCAP* **1510** (2015) 10, 068, [arXiv:1505.04866 [astro-ph.HE]].

- [17] M. G. Aartsen *et al.* [IceCube Collaboration], “Search for Dark Matter Annihilation in the Galactic Center with IceCube-79,” *Eur. Phys. J. C* **75** (2015) 10, 492, [arXiv:1505.07259 [astro-ph.HE]].
- [18] K. Frankiewicz [Super-Kamiokande Collaboration], “Searching for Dark Matter Annihilation into Neutrinos with Super-Kamiokande,” arXiv:1510.07999 [hep-ex].
- [19] I.A. Belolaptikov *et al.* [Baikal Collab.], “The Baikal underwater neutrino telescope: Design, performance and first results”, *Astropart.Phys.* 7 (1997) 263.
- [20] V.M. Aynutdinov *et al.* [Baikal Collab.], “Baikal neutrino telescope”, *Phys.Atom.Nucl.* 69 (2006) 1914.
- [21] A.D.Avrorin *et al.* [Baikal Collab.], “Baikal-GVD: first cluster Dubna”, *PoS EPS-HEP2015* (2015), arXiv:1511.02324[physics.ins-det].
- [22] A. D.Avrorin *et al.* [Baikal Collab.], “Status and recent results of the BAIKAL-GVD project”, *Phys. Part. Nucl.* 46 (2015) 2, 211.
- [23] A.D.Avrorin *et al.* [Baikal Collab.], “Sensitivity of the Baikal-GVD neutrino telescope to neutrino emission toward the center of the galactic dark matter halo”, *JETP Lett.* 101 (2015) 5, 289, arXiv:1412.3672 [astro-ph.HE].
- [24] V. Aynutdinov *et al.* [Baikal Collab.], “The Baikal Neutrino experiment: Status, selected physics results, and perspectives,” *Izvestia Akademii Nauk (Izvestia Russ. Academy Science)*, Ser. Phys., vol. 71, N.4, 2007.
- [25] V.M. Aynutdinov *et al.* [Baikal Collab.], “Search for relativistic magnetic monopoles with the Baikal Neutrino Telescope”, *Astropart.Phys.* 29 (2008) 366.
- [26] V. Aynutdinov *et al.* [Baikal Collab.], “The BAIKAL neutrino experiment: Physics results and perspectives,” *Nucl. Instrum. Methods, vol A602*, (2009), 14.
- [27] A.V. Avrorin *et al.* [Baikal Collab.], “Search for neutrinos from Gamma-Ray Bursts with the Baikal Neutrino Telescope NT200,” *Astronomy Lett.* V.37, N.10 (2011) 692.
- [28] A.V. Avrorin *et al.* [Baikal Collab.], “Search for astrophysical neutrinos in the Baikal neutrino project,” *Phys.Part.Nucl.Lett.* 8 (2011) 704.
- [29] A. D. Avrorin *et al.* [Baikal Collaboration], “Search for neutrino emission from relic dark matter in the Sun with the Baikal NT200 detector,” *Astropart. Phys.* **62** (2014) 12, [arXiv:1405.3551 [astro-ph.HE]].
- [30] D. Heck *et al.*, Forschungszentrum Karlsruhe, Technical Report No. 6019, 1998.
- [31] E. Bugaev, S. Klimushin, I. Sokalsky, *Phys. Rev. D*, vol. 64, p. 074015, 2001.
- [32] V. Agrawal, T. Gaisser, P. Lipari and T. Stanev, “Atmospheric neutrino flux above 1 GeV,” *Phys. Rev.*, vol. D53, p. 1314, 1996.
- [33] I. A. Belolaptikov, Preprint of INR RAS 1178/2007 (in Russian), 2007, also see at [https://www-zeuthen.desy.de/wischnew/baikal/publications/baikal2007/nu mc sel preprint.pdf](https://www-zeuthen.desy.de/wischnew/baikal/publications/baikal2007/nu_mc_sel_preprint.pdf).
- [34] J. F. Navarro, C. S. Frenk and S. D. M. White, “The Structure of cold dark matter halos,” *Astrophys. J.* **462** (1996) 563.
- [35] J. F. Navarro, C. S. Frenk and S. D. M. White, “A Universal density profile from hierarchical clustering,” *Astrophys. J.* **490** (1997) 493.
- [36] A. V. Kravtsov, A. A. Klypin, J. S. Bullock and J. R. Primack, “The Cores of dark matter dominated galaxies: Theory versus observations,” *Astrophys. J.* **502** (1998) 48.
- [37] B. Moore, S. Ghigna, F. Governato, G. Lake, T. R. Quinn, J. Stadel and P. Tozzi, “Dark matter substructure within galactic halos,” *Astrophys. J.* **524** (1999) L19.
- [38] A. Burkert, “The Structure of dark matter halos in dwarf galaxies,” *IAU Symp.* **171** (1996) 175. [*Astrophys. J.* **447** (1995) L25].
- [39] M. Kuhlen, M. Vogelsberger and R. Angulo, “Numerical Simulations of the Dark Universe: State of the Art and the Next Decade,” *Phys. Dark Univ.* **1** (2012) 50, [arXiv:1209.5745 [astro-ph.CO]].
- [40] V. S. Berezhinsky, V. I. Dokuchaev and Y. N. Eroshenko, “Small-scale clumps of dark matter,” *Phys. Usp.* **57** (2014) 1 [*Usp. Fiz. Nauk* **184** (2014) 3], [arXiv:1405.2204 [astro-ph.HE]].
- [41] F. Nesti and P. Salucci, “The Dark Matter halo of the Milky Way, AD 2013,” *JCAP* **1307** (2013) 016.
- [42] P. Baratella, M. Cirelli, A. Hektor, J. Pata, M. Pöbbeleht and A. Strumia, “PPPC 4 DM $\nu$ : A Poor Particle Physicist Cookbook for Neutrinos from DM annihilations in the Sun,” arXiv:1312.6408 [hep-ph].
- [43] D. V. Forero, M. Tortola and J. W. F. Valle, “Neutrino oscillations refitted,” *Phys. Rev. D* **90** (2014) 093006, [arXiv:1405.7540 [hep-ph]].
- [44] M. M. Boliev, S. V. Demidov, S. P. Mikheyev and O. V. Suvorova, “Search for muon signal from dark matter annihilations in the Sun with the Baksan Underground Scintillator Telescope for 24.12 years,” *JCAP* **1309** (2013) 019, [arXiv:1301.1138 [astro-ph.HE]].
- [45] G. C. Hill and K. Rawlins, “Unbiased cut selection for optimal upper limits in neutrino detectors: The Model rejection potential technique,” *Astropart. Phys.* **19** (2003) 393, [astro-ph/0209350].
- [46] Wolfgang A. Rolke, Angel M. Lopez, Jan Conrad, “Limits and confidence intervals in the presence of nuisance parameters,” *Nucl.Instrum.Meth.* **A551** (2005) 493.
- [47] <http://root.cern.ch> R. Brun *et al.*, *Nucl. Instrum. Methods in Phys. Res.*, 1996.
- [48] V. Aynutdinov *et al.* [Baikal Collaboration], “Search for a diffuse flux of high-energy extraterrestrial neutrinos with the NT200 neutrino telescope,” *Astropart. Phys.* **25**, (2006) 140.
- [49] S. S. Wilks, “The Large-Sample Distribution of the Likelihood Ratio for Testing Composite Hypotheses,” *Annals Math. Statist.* **9** (1938) 1, 60.
- [50] K. A. Olive *et al.*, [Particle Data Group Collaboration], “Review of Particle Physics,” *Chin. Phys. C* **38** (2014) 090001.
- [51] A. Cooper-Sarkar, P. Mertsch and S. Sarkar, “The high energy neutrino cross-section in the Standard Model and its uncertainty,” *JHEP* **1108** (2011) 042, [arXiv:1106.3723 [hep-ph]].
- [52] R. Catena and P. Ullio, “A novel determination of the local dark matter density,” *JCAP* **1008** (2010) 004, [arXiv:0907.0018

- [astro-ph.CO]].
- [53] F. S. Queiroz, C. E. Yaguna and C. Weniger, “Gamma-ray Limits on Neutrino Lines,” arXiv:1602.05966 [hep-ph].
  - [54] A. Drlica-Wagner *et al.* [Fermi-LAT and DES Collaborations], “Search for Gamma-Ray Emission from DES Dwarf Spheroidal Galaxy Candidates with Fermi-LAT Data,” *Astrophys. J.* **809** (2015) 1, L4, [arXiv:1503.02632 [astro-ph.HE]].
  - [55] B. Zitzer [VERITAS Collaboration], “Search for Dark Matter from Dwarf Galaxies using VERITAS,” arXiv:1509.01105 [astro-ph.HE].
  - [56] J. Aleksic *et al.*, “Optimized dark matter searches in deep observations of Segue 1 with MAGIC,” *JCAP* **1402** (2014) 008, [arXiv:1312.1535 [hep-ph]].
  - [57] A. Abramowski *et al.* [HESS Collaboration], “Search for dark matter annihilation signatures in H.E.S.S. observations of Dwarf Spheroidal Galaxies,” *Phys. Rev. D* **90** (2014) 112012, [arXiv:1410.2589 [astro-ph.HE]].
  - [58] M. G. Aartsen *et al.* [IceCube Collaboration], “The IceCube Neutrino Observatory - Contributions to ICRC 2015 Part IV: Searches for Dark Matter and Exotic Particles,” arXiv:1510.05226 [astro-ph.HE].
  - [59] P. Meade, M. Papucci, A. Strumia and T. Volansky, “Dark Matter Interpretations of the  $e^+$  Excesses after FERMI,” *Nucl. Phys. B* **831** (2010) 178, [arXiv:0905.0480 [hep-ph]].
  - [60] O. Adriani *et al.* [PAMELA Collaboration], “An anomalous positron abundance in cosmic rays with energies 1.5-100 GeV,” *Nature* **458** (2009) 607, [arXiv:0810.4995 [astro-ph]].
  - [61] A. A. Abdo *et al.* [Fermi-LAT Collaboration], “Measurement of the Cosmic Ray  $e^+$  plus  $e^-$  spectrum from 20 GeV to 1 TeV with the Fermi Large Area Telescope,” *Phys. Rev. Lett.* **102** (2009) 181101, [arXiv:0905.0025 [astro-ph.HE]].
  - [62] F. Aharonian *et al.* [HESS Collaboration], “The energy spectrum of cosmic-ray electrons at TeV energies,” *Phys. Rev. Lett.* **101** (2008) 261104, [arXiv:0811.3894 [astro-ph]].
  - [63] G. Steigman, B. Dasgupta and J. F. Beacom, “Precise Relic WIMP Abundance and its Impact on Searches for Dark Matter Annihilation,” *Phys. Rev. D* **86** (2012) 023506, [arXiv:1204.3622 [hep-ph]].
  - [64] N. Bernal, J. E. Forero-Romero, R. Garani and S. Palomares-Ruiz, “Systematic uncertainties from halo asphericity in dark matter searches,” *JCAP* **1409** (2014) 004, [arXiv:1405.6240 [astro-ph.CO]].